

Determination of bone age using deep convolutional neural networks

 Fatih Ahmet Senel¹,  Ahmet Dursun²,  Kenan Ozturk²,  Veysel Atilla Ayyildiz³

¹Department of Computer Engineering, Faculty of Engineering, Suleyman Demirel University, Isparta, Turkey

²Department of Anatomy, Faculty of Medicine, Suleyman Demirel University, Isparta, Turkey

³Department of Radiology, Faculty of Medicine, Suleyman Demirel University, Isparta, Turkey

Copyright@Author(s) - Available online at www.annalsmedres.org

Content of this journal is licensed under a Creative Commons Attribution-NonCommercial 4.0 International License.



Abstract

Aim: Bone age assessment is an important measure of skeletal maturity in children with a growth development disorder. Furthermore, age estimation is an important method applied in various situations such as growth observation, immigrant registration, legal criminal justice, and body detection. In this study, we aimed to develop a computer-assisted bone age detection system.

Materials and Methods: This detection is usually evaluated by a trained physician using a radiological examination of the left wrist and a reference model. However, this evaluation method was stated to cause differences brought by interobserver and intraobserver variabilities. Several automated approaches have been proposed to overcome these problems, but none of them have been proven to be generalized according to different races, age ranges, and gender. Considering today's technology, it is observed that developments in the software are already used in the field of health. In this study, bone age was determined from X-rays of the left wrist using convolutional neural networks, which are a popular subject of recent years.

Results: In the study, in which a total of 150 patients' images were used, different deep learning architectures were used and the results were compared. On average, the success rate was best at 98.39% with different training-testing split rates.

Conclusion: This study demonstrated that deep learning could be used to determine bone age.

Keywords: Age estimation; deep learning; greulich and Pyle; X-ray of the wrist

INTRODUCTION

Bone age assessment is a procedure used in both diagnostic and therapeutic investigations of endocrinology problems and genetic disorders in pediatric radiology (1). In recent years, due to the increase in migration and refugee flows and legal problems increasing depending on them, age estimation has become more critical. One of the essential issues of forensic medical applications is to ask for the age determination with regard to cases whose identity is unknown and whose age is suspected. Particularly, not knowing whether the population records of refugees are kept regularly or not creates problems with the actual age of persons. In terms of the criminal law and civil law of many countries, it is crucial that people have criminal and legal capacity. Age determination may be requested in cases such as criminal liability, marriage, and starting to work.

Since the bone ossification stages of the non-dominant hand are distinctive, it is usually performed by the radiological examination of the left wrist and then compared with chronological age. Inconsistency between

the two values indicates abnormalities. The analysis of X-ray radiographs of the left wrist is widely used in the assessment of bone maturity due to its simplicity, minimal radiation exposure, and the presence of multiple ossification centers (1). The reason for using the left wrist is that most people use the right wrist and the right wrist is more likely to be injured than the left wrist. Furthermore, an agreement was reached at the meeting of physical anthropologists at the beginning of the 20th century, and it was determined that physical measurements should be made on the left side of the body (2). Various methods have been used to determine the radiological bone age. The most commonly used methods are the Greulich and Pyle atlas (GP) and the Tanner-Whitehouse method (TW), both of which are performed by evaluating X-ray radiographs of the left wrist (2). In the Greulich and Pyle atlas method, the expert compares the hand radiography of an individual with a series of standard images in the atlas. The most similar image is selected, and the bone age of the individual is determined according to this image (3). Simplicity and speed in determining bone age have made this atlas the most popular method. However, this approach

Received: 25.08.2020 **Accepted:** 30.09.2020 **Available online:** 09.07.2021

Corresponding Author: Fatih Ahmet Senel, Department of Computer Engineering, Faculty of Engineering, Suleyman Demirel University, Isparta, Turkey **E-mail:** fatihsenel@sdu.edu.tr

is very subjective. In some studies, inter-observer reading differences varied between 0.37 and 0.6 years, and intra-observer reading differences were reported to be between 0.25 and 0.96 years (3). The Tanner-Whitehouse method is a more subjective method, and bone age is calculated from the sum of the developmental scores of twenty ossification centers. This approach is less preferred since it is both complex and time-consuming (3).

Undoubtedly, an area in which advancements are taking place with the developing technology is also the health sector. The benefits of all kinds of technological developments are also observed in the field of health. With the active introduction of artificial intelligence into our lives, the use of machines is becoming widespread with the elimination of human factors in many areas. Deep learning is gradually increasing its popularity with today's developing equipment. Artificial neural networks, in which hardware resources are insufficient, have evolved into the use of deep neural networks by passing to the next level with the development of hardware technology. The deep learning method allows studies on the subjects of image processing, eliminates the difficulties of classical image processing techniques, and provides the opportunity to achieve better results practically. Nowadays, the areas of usage of deep learning continue to increase (4-9).

The skeletal maturation rate is sensitive to environmental impacts at both the individual and population levels. Differences in the rate and timing of skeletal maturity are affected by differences such as nutrition, environment, socioeconomic status, and genetics (10). In order to eliminate the effects of these differences in our study, we created our own data set and conducted our study on our own data set. Thus, we aimed to develop a system that can be used actively in small societies that can be created with fewer data sets and can be used for bone age determination.

MATERIALS and METHODS

Creation of the Data Set and Preprocessing

Our study was carried out on a total of 150 left wrist X-ray radiographs of 114 male and 36 female patients, in the age range from zero to 18 years, taken from the PACS (Picture Archiving and Communication Systems) system of the Faculty of Medicine Research and Application Hospital. The X-ray images were evaluated by using the "RadiAnt DICOM viewer 4.6.9 version."

The images were evaluated twice at different times by two different specialist physicians (A radiologist and an anatomist), and the mean bone age values were accepted as the bone age of the patients, and cases were labeled in this way. In X-ray radiographic evaluations, the Greulich and Pyle atlas was based on. There were no differences between chronological age and bone age in 72 of the 150 cases. The bone age was determined to be higher than chronological age in 46 cases, and the mean difference between bone age and chronological age was 1.13 years.

The bone age was found to be lower than chronological age in 32 cases, and the mean difference between bone age and chronological age was 1.19 years.

After creating the data set, the necessary cropping procedures were performed on all X-ray images in a way that only the left wrist would be left. The cropping process was performed due to the presence of materials that are superposed into images such as the hand of the parent, direction materials, buttons, and medical devices such as catheters, and similar materials. The sample X-ray images in the data set are presented in Figure 1.

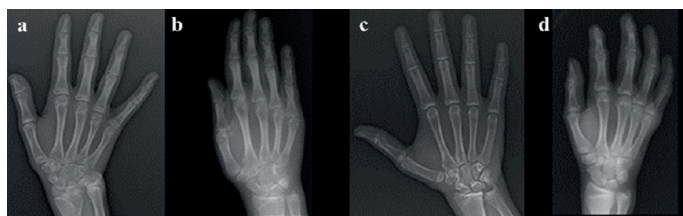


Figure 1. Data set sample X-ray images (a) 12-year-old (chronological) female (b) 15-year-old (chronological) female (c) 15-year-old (chronological) male (d) 17-year-old (chronological) male

Data Augmentation

In order to increase the success of deep learning, a large number of samples should be given to the deep neural network. Because of advantages of the large size of the data set, there are methods developed to increase the number of data sets in studies conducted with deep learning. Some of them are methods such as rotating images, taking their reflections, changing brightness values, scaling, shifting, adding noise, etc. (11). In this study, to extend the data set, the data set size was increased by 12 times using the rotation, reflection, scaling and shifting techniques. The number of images, which was 150 in total, was increased, and 1800 images were obtained.

The Deep Learning Architectures Used

In this study, three convolutional neural network architectures which were used frequently and tested successfully in the literature were used.

1. AlexNet

The AlexNet deep learning architecture, which was developed by Krizhevsky et al. (12), won the ImageNet competition in 2012, and since it yields successful results in many applications, it is still being used nowadays. The AlexNet architecture consists of 25 layers, and 11x11 size filters are used in its structure. It receives images of 227x227x3 in size as input.

2. GoogleNet

GoogleNet is the deep learning architecture, which was developed by Szegedy et al. and won the 2014 ImageNet competition (13). The GoogleNet architecture, which has a depth of 22 layers, consists of filters of 1x1, 3x3, 5x5, and 7x7 in size. Furthermore, it includes dropout and max-pooling layers in its structure and receives images of 224x224x3 in size as input.

3. Vgg19

The Vgg19 deep learning architecture was developed by the Oxford University Visual Geometry Group as a continuation of the Vgg16 architecture (14-15). There are a total of 47 layers in its structure. The input image sizes are 224x224x3.

Metrics

Three different metrics were used to compare the success of the methods used in this study. These are Mean Squared Error (MSE), Mean Absolute Error (MAE), and Accuracy (Acc) metrics. The calculation of MAE, MSE, and Acc metrics is given in Equation 1, Equation 2, and Equation 3, respectively.

$$MAE = \frac{1}{n} \sum_{i=1}^n |y'_i - y_i| \quad (1)$$

$$MSE = \frac{1}{n} \sum_{i=1}^n (y'_i - y_i)^2 \quad (2)$$

$$Acc = \frac{C}{A} \quad (3)$$

Here, n represents the number of samples, y'_i represents the estimated output, and y_i represents the actual output value. C represents the number of correctly classified samples, and A represents the number of all samples.

RESULTS

In this study, the process of estimating bone ages on X-ray images of the left wrists of people in the age range of 0-18 years and with mixed male/female distribution was performed with deep learning. The results were obtained by using three deep learning architectures. The AlexNet, GoogleNet, and Vgg19 architectures have been used in many different studies in the literature (11,16-22). By considering their success, they were preferred to be used in this study.

While the experiments were carried out, the whole data set was evaluated for three different situations as training and testing data sets. Each classification process was run 10 times. The classifiers were compared according to the average results. Training and testing data sets were separated as 90%-10%, 80%-20%, and 70%-30%, and the results were obtained for each situation.

Table 1. Performance comparisons of the classifiers

Classifier	Training-Testing Data Splitting	Metrics	Min	Max	Mean
GoogleNET	70%-30%	MSE	0.0051	0.0108	0.0072
		MAE	0.0078	0.0152	0.0107
		Acc	0.8627	0.9369	0.9137*
	80%-20%	MSE	0.0010	0.0157	0.0046
		MAE	0.0024	0.0233	0.0077
		Acc	0.7972	0.9917	0.9406*
	90%-10%	MSE	0.0001	0.0047	0.0013
		MAE	0.0009	0.0085	0.0029
		Acc	0.9389	1.0000	0.9839*
AlexNET	70%-30%	MSE	0.0086	0.0209	0.0148
		MAE	0.0134	0.0304	0.0204
		Acc	0.7291	0.8942	0.8199
	80%-20%	MSE	0.0066	0.0119	0.0090
		MAE	0.0099	0.0158	0.0128
		Acc	0.8556	0.9333	0.8942
	90%-10%	MSE	0.0037	0.0089	0.0064
		MAE	0.0048	0.0131	0.0100
		Acc	0.9000	0.9611	0.9228
Vgg19	70%-30%	MSE	0.0213	0.0263	0.0235
		MAE	0.0280	0.0337	0.0300
		Acc	0.6883	0.7458	0.7263
	80%-20%	MSE	0.0156	0.0189	0.0172
		MAE	0.0206	0.0237	0.0217
		Acc	0.7806	0.8139	0.8009
	90%-10%	MSE	0.0117	0.0133	0.0125
		MAE	0.0157	0.0167	0.0163
		Acc	0.8444	0.8556	0.8481

MSE: Mean squared error, MAE: Mean absolute error, Acc: Accuracy (the ratio of the number of correctly classified samples to all samples)
* the best classification result

When comparing the results, firstly, the Acc data were taken into consideration, and in case of an equality of the Acc data, the performances of the classifiers were compared by considering the MAE and MSE values. The obtained experimental results are presented in Table 1.

When the results in Table 1 are examined, the best classification result was observed with GoogleNET architecture. GoogleNET architecture came first in all 3 different training-testing split rates. When the other two methods are compared, the AlexNET architecture is better than the Vgg19 architecture. The GoogleNET architecture was able to achieve a successful classification of 100% in 90%-10% training-testing split rate.

When comparing MSE and MAE values, it is understood that the GoogleNET architecture is decisively ahead. The convergence graphics along the iteration steps are given in Figure 2,3 and 4. The figures show that the GoogleNET classifier has achieved better results than the other two methods as from the first iteration step.

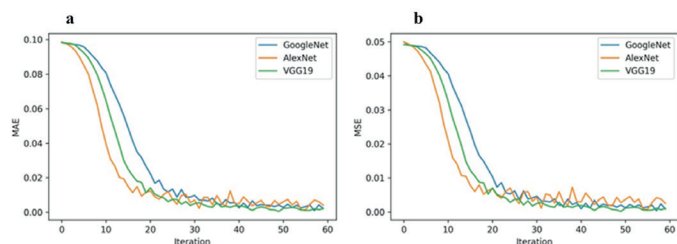


Figure 2. Metric values of experimental results according to iterations (a) 90%-10% Training-Testing Data Splitting MAE (Mean absolute error) graphic (b) 90%-10% Training-Testing Data Splitting MSE (Mean squared error) graphic

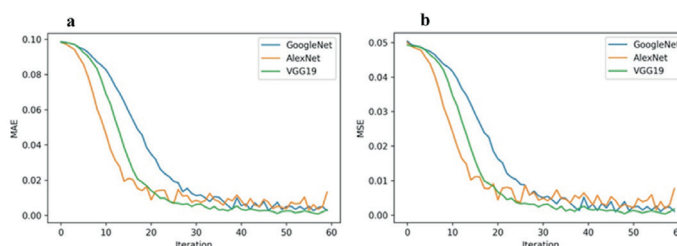


Figure 3. Metric values of experimental results according to iterations (a) 80%-20% Training-Testing Data Splitting MAE (Mean absolute error) graphic (b) 80%-20% Training-Testing Data Splitting MSE (Mean squared error) graphic

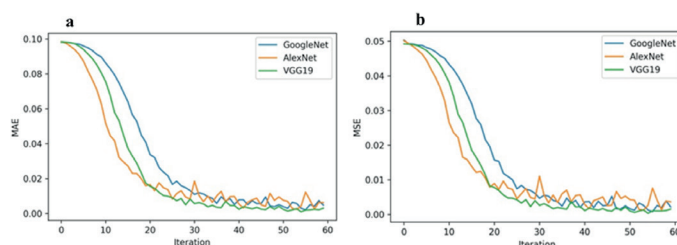


Figure 4. Metric values of experimental results according to iterations (a) 70%-30% Training-Testing Data Splitting MAE (Mean absolute error) graphic (b) 70%-30% Training-Testing Data Splitting MSE (Mean squared error) graphic

DISCUSSION

Sexual maturation, chronological age, weight, height, tooth development and skeletal development characteristics are used to determine the stages of growth. It is extremely important to determine maturation before or during puberty and to evaluate subsequent growth potential (23). Bone age assessment is required in many medical situations and also for asylum-seeker rights, in which age is important, within the legal contexts. However, the current bone age estimation procedures are time-consuming. The GP atlas appears as a relevant collection of indicators for skeletal development of modern populations. However, the natural variation around the mean for a population is substantial and must be taken into account when the atlas is used (24). The observed heterogeneity between different populations and studies has been a topic of discussion for decades, and explanatory models include regional genetic heterogeneity (25-27) as well as extrinsic factors such as nutritional status (28), socioeconomic factors and body mass index (29). The fact that the radiographs are interpreted manually and based on subjective judgment certainly opens the possibility of measurement error. Furthermore, in some studies, inter-observer reading differences ranged from 0.37 to 0.6 years, and intra-observer reading differences were reported to be between 0.25 and 0.96 years (3).

In this study, a deep learning system was developed for the prediction of bone age on the X-rays of the left wrist. Different studies have been performed on the detection of bone age. Larson et al. (30) performed bone age estimation with the deep learning system by using X-ray images of the wrists. In order to test the estimation model they developed, they made comparisons with the evaluation results of three different experts and with the digital atlas. As a result, with the estimation of the system they obtained, they achieved a zero-age difference on a yearly basis with both the digital atlas and expert results. In other words, they were able to achieve the same results with deep learning. The system they developed achieved closer results to people. Using the RSNA2017 Pediatric Bone Age database, Chu et al. (31) developed the age estimation process from wrist images of children in the 0-19 age group with a two-stage deep learning system. In the system they developed, in the first stage, a network structure masks the wrist in images, and then age estimation is performed by focusing only on the wrist with this mask. They achieved a successful result with an error rate of 5.98 months. Lee et al. (32) aimed to estimate bone age based on children's wrist X-ray images of the 5-18 age group. They did not include those at four years of age and younger in their studies due to limited radiological images. Accordingly, they obtained their results at an accuracy rate of 92.29% for detection with a one-year error rate and at an accuracy rate of 98.56% for detection with a two-year error rate. Using the RSNA2017 Pediatric Bone Age database, Iglovikov et al. (33) developed a deep learning system that could detect bone age. Firstly, they

developed a system to be able to mask only the areas of images that should be focused on. They divided the wrist images into three regions (whole hand, the carpal region of the hand, metacarpals and proximal phalanges) and performed bone age estimation with regionally different deep learning systems. They obtained the most successful results by evaluating the three regions together.

In this study, bone age estimation was performed with deep learning algorithms. Based on the X-Ray images of the left wrist of 150 different patients in total, age estimation was performed at a success rate of 98.39% with 90%-10% training-testing split. Considering the environmental and genetic effects on bone age, we think that being able to perform age estimation at a success rate of 98.39% in our study will enable the use of deep learning in the estimation of bone age in smaller societies. We believe that this study has contributed to the literature during this period when bone age estimation is of great importance, and the adaptation of technological developments to the field of health is almost mandatory.

There were some limitations to this study. The cases included in the study were those who were admitted to the hospital for various reasons and had radiographs of the left wrist. Therefore, the results may not accurately reflect healthy individuals. Also, the small sample size is a limitation of this study. However, this study achieved a high accuracy rate in estimating bone age.

The effects of gender on hand and wrist shape and gender-related differences have been studied using different methods (34,35). Several studies have found a significant difference between men's and women's hand bones (34,35). Bone age in females progresses at all ages compared to males, and this difference is slightly more pronounced after the onset of puberty, and therefore skeletal maturation of males takes longer than females (36). Koc et al. (23) in their study, the difference between genders was found mostly in the radiocarpal region. The number of female participants in our study was limited. In this case, it may affect the accuracy of the results of the deep learning algorithm created on the left wrist graphics of women.

For age estimation, in addition to wrist X-ray, other radiological examinations are also used. X-ray images of different body regions such as elbows, shoulders, clavicle, teeth, crista iliaca, and knees are the main radiological methods used to estimate the bone age of individuals (37). Whether a person is over the age of 18 is critical since it will change the judging system in most countries. At this age threshold, hand radiographs are not useful since bone structures on hand radiographs have completed their development. Therefore, in the forensic age estimation of 18 years and above, it is recommended to evaluate the epiphyses that may be still open, such as the medial clavicle epiphysis (37). Furthermore, X-ray exposure in direct radiographs has led to the coming of other radiological examinations such as ultrasonography (US)

and magnetic resonance imaging (MRI) into prominence (37). In recent years, due to the increase in migration and refugee flows and the increasing legal problems due to these, age estimation has become more critical. When it is considered that racial, environmental, and socioeconomic differences also affect age determination, it will be even more important to provide age estimation using the deep learning method by creating data sets, which are unique for that society, on the data obtained with X-Ray images of different body regions or with different radiological imaging methods. In future studies, we aim to use X-ray images of different regions and to use images obtained by different imaging techniques (such as US and MRI).

CONCLUSION

In this study, it was shown that bone age estimation can be made with deep learning method without the need for an experienced radiologist or specialist physician to determine bone age. The fact that the deep learning algorithm developed in our study can work with a small sample increases its usage area. In this way, the error rate that may be caused by differences between societies will be reduced. This method can provide an alternative in determining bone age.

Competing interests: The authors declare that they have no competing interest.

Financial Disclosure: There are no financial supports.

Ethical approval: This study was approved by Süleyman Demirel University School of Medicine Clinical Research Ethics Committee. (Decision number:380 and Decision date 23.12.2019).

REFERENCES

1. Spampinato C, Palazzo S, Giordano D, et al. Deep learning for automated skeletal bone age assessment in X-ray images. *Med Image Anal* 2017;36:41-51.
2. Pose Lepe G, Villacrés F, Fuente-Alba CS, et al. Correlation in radiological bone age determination using the Greulich and Pyle method versus automated evaluation using BoneXpert software. *Rev Chil Pediatr*. 2018;89:606-11.
3. Haghnegahdar A, Pakshir H, Ghanbari I. Correlation between Skeletal Age and Metacarpal Bones and Metacarpophalangeal Joints Dimensions. *J Dent* 2019;20:159-64.
4. Chen C, Liu Y, Kumar M, et al. Energy consumption modelling using deep learning embedded semi-supervised learning. *Comput Ind Eng* 2019;135:757-65.
5. Oh J, Yun K, Maoz U, et al. Identifying depression in the National Health and Nutrition Examination Survey data using a deep learning algorithm. *J Affect Disord* 2019;257:623-31.
6. Shen S, Sadoughi M, Chen X, et al. A deep learning method for online capacity estimation of lithium-ion batteries. *J Energy Storage* 2019;25:100817.
7. Wu L, Liu Z, Bera T, et al. A deep learning model to recognize food contaminating beetle species based on elytra fragments. *Comput Electron Agric* 2019;166:105002.

8. Yi PH, Kim TK, Wei J, et al. Automated semantic labeling of pediatric musculoskeletal radiographs using deep learning. *Pediatr Radiol* 2019;49:1066-70.
9. Zhu L, Zhang C, Zhang C, et al. Forming a new small sample deep learning model to predict total organic carbon content by combining unsupervised learning with semisupervised learning. *Appl Soft Comput* 2019;83:1055-96.
10. Cole TJ, Rousham EK, Hawley NL, et al. Ethnic and sex differences in skeletal maturation among the Birth to Twenty cohort in South Africa. *Arch Dis Child*. 2015;100:138-43.
11. Khan SU, Islam N, Jan Z, et al. A novel deep learning based framework for the detection and classification of breast cancer using transfer learning. *Pattern Recognit Lett* 2019;125:1-6.
12. Krizhevsky A, Sutskever I, Hinton GE. ImageNet Classification with Deep Convolutional Neural Networks. In: *NIPS'12: Proceedings of the 25th International Conference on Neural Information Processing Systems*. 2012;1097-105.
13. Szegedy C, Liu W, Jia Y, et al. Going deeper with convolutions. In: *Proceedings of the IEEE Computer Society Conference on Computer Vision and Pattern Recognition*. IEEE Computer Society 2015;1-9.
14. Simonyan K, Zisserman A. Very Deep Convolutional Networks for Large-Scale Image Recognition. *Comput Vis Pattern Recognit* 2014;1:1-14.
15. Zheng Y, Yang C, Merkulov A. Breast cancer screening using convolutional neural network and follow-up digital mammography. In: *Computational Imaging III*. San Francisco 2018;4.
16. Shanthi T, Sabeenian RS. Modified Alexnet architecture for classification of diabetic retinopathy images. *Comput Electr Eng* 2019;76:56-64.
17. Lu S, Lu Z, Zhang YD. Pathological brain detection based on AlexNet and transfer learning. *J Comput Sci* 2019;30:41-7.
18. Saikia AR, Bora K, Mahanta LB, et al. Comparative assessment of CNN architectures for classification of breast FNAC images. *Tissue Cell* 2019;57:8-14.
19. Deepak S, Ameer PM. Brain tumor classification using deep CNN features via transfer learning. *Comput Biol Med* 2019;111:103345.
20. Wan S, Liang Y, Zhang Y. Deep convolutional neural networks for diabetic retinopathy detection by image classification. *Comput Electr Eng* 2018;72:274-82.
21. Shallu, Mehra R. Breast cancer histology images classification: Training from scratch or transfer learning? *ICT Express* 2018;4:247-54.
22. Toraman S, Tuncer SA, Balgetir F. Is it possible to detect cerebral dominance via EEG signals by using deep learning? *Med Hypotheses* 2019;131:109315.
23. Koc U, Ercan I, Ozdemir S, et al. Statistical shape analysis of hand and wrist in paediatric population on radiographs. *Turk J Med Sci* 2020;50:1288-97.
24. Dahlberg PS, Mosdøl A, Ding Y, et al. A systematic review of the agreement between chronological age and skeletal age based on the Greulich and Pyle atlas. *Eur Radiol* 2019;29:2936-48.
25. Mansourvar M, Ismail MA, Raj RG, et al. The applicability of Greulich and Pyle atlas to assess skeletal age for four ethnic groups. *J Forensic Leg Med* 2014;22:26-9.
26. Mora S, Boechat MI, Pietka E, et al. Skeletal Age determinations in children of European and African descent: applicability of the Greulich and Pyle standards. *Pediatr Res* 2001;50:624-8.
27. Zhang A, Sayre JW, Vachon L, Liu BJ, Huang HK. Racial differences in growth patterns of children assessed on the basis of bone age. *Radiology* 2009;250:228-35
28. Fleshman K. Bone age determination in a paediatric population as an indicator of nutritional status. *Trop Doct* 2000;30:16-8
29. Chaumoitre K, Lamtali S, Baali A, et al. Influence of socioeconomic status and body mass index on bone age. *Horm Res Paediatr* 2010;74:129-35
30. Larson DB, Chen MC, Lungren MP, et al. Performance of a deep-learning neural network model in assessing skeletal maturity on pediatric hand radiographs. *Radiology* 2018;287:313-22.
31. Chu M, Liu B, Zhou F, et al. Bone Age Assessment Based on Two-Stage Deep Neural Networks. *Int Conf Digit Image Comput Tech Appl DICTA* 2018;1-6.
32. Lee H, Tajmir S, Lee J, et al. Fully Automated Deep Learning System for Bone Age Assessment. *J Digit Imaging* 2017;30:427-41.
33. Iglovikov VI, Rakhlin A, Kalinin AA, et al. Paediatric bone age assessment using deep convolutional neural networks. *Lect Notes Comput Sci* 2018;11045.
34. Schneider MT, Zhang J, Crisco JJ, et al. Men and women have similarly shaped carpometacarpal joint bones. *J Biomechanics* 2015;48:3420-6.
35. Didi ALM, Azman RR, Nazri M. Sex determination from carpal bone volumes: A Multi Detector Computed Tomography (MDCT) study in a Malaysian population. *Legal Med* 2016;20:49-52.
36. Mora S, Boechat MI, Pietka E, et al. Skeletal age determinations in children of European and African descent: applicability of the Greulich and Pyle standards. *Pediatric Research* 2001;50:624-8.
37. Yeniceri IO, Tosun K. Can relative area of medial clavicular epiphysis be used for age estimation? *J For Med*. 2017;31:53-8.